AIAA AVIATION Forum
13-17 June 2016, Washington, D.C.
16th AIAA Aviation Technology, Integration, and Operations Conference

10.2514/6.2016-3463

The Effects of Supersonic Inlet Topology on the Installed Performance of Turbofan Engines

Ryan M. Palma[1] and Timothy T. Takahashi[2]
Arizona State University, Tempe, Arizona, 85287

This study explores the system level design impacts of differing supersonic inlet topology. Historically, for Mach 2 flight, variable ramp angle external compression inlets have been preferred over normal shock inlets on the basis of pressure recovery. However, from a system design perspective, is inlet pressure recovery everything? We compare a variety of low-bypass ratio turbofan engines, modelled with NASA's *Numerical Propulsion System Integration* (*NPSS*), that can propel a F-16-inspired tactical fighter aircraft. We compute installed performance by applying installation limits (buzz and distortion) and losses (bleed, bypass, spillage, and total pressure recovery) as suggested by the USAF *Performance of Installed Propuslion Systems* (*PIPSI*) protocol. Our design study matrix comprises three different engines (Bypass Ratio of 0.5, 1.0, and 1.5) matched to one of three inlet topologies (normal shock, fixed ramp external compression and variable ramp external compression) scaled to any of five possible capture areas. We found that the variable ramp external compression inlet was unforgiving of higher bypass ratio engines. Compared to the robust nature of the normal shock inlet leads the authors to believe that the normal shock inlet, not the complex variable geometry ramp inlet, may be the superior choice for many supersonic propulsion design applications.

Nomenclature

A_∞	=	Actual Inlet Capture Area (Freestream conditions) representing the flow through the inlet, ft^2
A_c	=	Reference Area of Flow that passes through the Inlet, the "highlight area," ft^2
AB	=	Afterburner
C_D	=	Total Drag Coefficient (normalized on Reference Capture Area, *Ac*)
BPR	=	Bypass Ratio
CD_{spill}	=	Spill Drag Coefficient (normalized on Reference Capture Area, *Ac*)
CD_{bleed}	=	Bleed Drag Coefficient (normalized on Reference Capture Area, *Ac*)
CD_{bypass}	=	Bypass Drag Coefficient (normalized on Reference Capture Area, *Ac*)
D	=	Total Drag Force, lbf
FPR	=	Fan Pressure Ratio
M	=	Mach Number
MFR	=	Mass Flow Ratio (ratio of bypass duct mass flow to core mass flow)
OPR	=	Overall Pressure Ratio
PLA	=	Power Lever Angle
p_t	=	Total Pressure, lbf/ft^2
P_s	=	Specfic Excess Power
ROC	=	Rate of Climb, ft/min
SR	=	Specific Range, nm/lbf
T	=	Thrust, lbf
TIT	=	Turbine Inlet Temperature, °R
tsfc	=	Thrust-Specific-Fuel-Consumption, lbm/(lbf-hr)
V_{ktas}	=	Knots True Airspeed, nm/hr

[1] M.S. Candidate, Aerospace Engineering, Arizona State University, AIAA Student Member
[2] Professor of Practice, Aerospace Engineering, Arizona State University, P.O. Box 876106, Tempe, AZ. Associate Fellow AIAA.

W = Weight, lbm
$\dot{W}_{eng}$ = Engine Weight Flow, lbm/sec
$\dot{W}_{ideal}$ = Ideal Weight Flow supplied by the inlet, lbm/sec
γ = Specific Heat Ratio

I. Introduction

AIRCRAFT DESIGN can appear to be more of an art than a science. Almost every deisgn choice affects and depends on another. This leads the designer to face a large multivariable modelling and simulation problem. Just the smallest change to wing thickness, wing span, or even wing placement along the fuselage can have huge ramifications to the aerodynamic performance of the aircraft, as well as its stability. Similarly, small changes in engine cycle or inlet technology may have huge impacts upon the performance envelope of the aircraft. Therefore, it is imperative that no design is left off the table before it can be analyzed for the mission. Doing so could result in a subpar aircraft, or even an unflyable one.

We can apply a multi-disciplinary modelling and simulation approach to the preliminary design of the propulsion system of a supersonic aircraft. Thrust, is one of the most important aspects of an aircraft design. Without thrust an airplane would be unable to fly even if it was otherwise perfectly designed. In this paper, we will show how poorly "installed" propulsion systems (mismatched engines and inlets) can lead to major problems in the performance of the overall airplane, to the point that the airplane would be unable to fly at many speeds and/or altitudes.

These problems are especially important for supersonic airplane design. Propulsion system design becomes especially complicated as the aerodynamics of propulsion may become more important than the thermodynamics of propulsion. Consequently, during preliminary design it is important to exhaustively study all possible inlet design options in the context of a specific proposed thermodynamic. We are fortunate that the USAF reached out to the Boeing Company to develop a comprehensive database of all possible inlets.[1,2,3,4] We can link aerodynamic performance analysis tools[5] to a rapid numerical modelling system comprising a high-fidelity aerodynamic model of propulsion (through *PIPSI*)[1,2,3,4] as well as a realistic thermodynamic model of propulsion (through *NPSS*).[6]

Most supersonic inlets employ some form of external compression to slow down the airflow from freestream to the low subsonic speeds found at the engine face. Engineers developed several distinct design strategies: 1) inlets that decelerate supersonic flow to subsonic speeds through a strong detached normal shock, as opposed to 2) inlets that decelerate supersonic flow to subsonic speeds through a series of oblique shocks followed by a weak normal shock. For the second class of designs, the oblique shocks may be triggered by either a simple, fixed ramp or a complex, variable angle ramp system. Outside the scope of this paper, engineers have also successfully designed "mixed" internal/external compression inlets for aircraft like the SR-71; in these designs the terminal normal shock wave forms inside the throat.[7]

Each design strategy yields a possible choice for the propulsion system. However, it is the designer's goal to determine the inlet type and size along with the gas-turbine propulsion system specification that yields the "best" overall design. From a theoretical standpoint, for flight at higher supersonic speeds, the logical choice would be the variable ramp geometry external compression inlet; this topology exhibits superior pressure recovery characteristics.[4] However, a large number of aircraft do not use this approach even though it is an idea that has been around well before they were created.[8] For example, both the Vought F-8 Crusader and the General Dynamics F-16 both use fixed normal shock inlets. At first glance, it may appear that the designers were trying to save on cost and keep the simple, cheaper inlet design. Sóbester's notes that the normal shock inlet would have been the optimum configuration seeing as the variable geometry inlet would have caused a 4% acceleration penalty as well as a 7% decrease in turn rate at Mach 1.2.[8] This leads us to believe that there may be more to the supersonic inlet design than simply maximizing pressure recovery.

The goal of this paper then is to continue the work previously done by Gedeon &Takahashi[9,10,11] and Dickman & Takahashi[12] in order to understand the behavior of these external compression inlets. We hope that this study helps to expand the open knowledge-base regarding the practical problems in supersonic propulsion airframe integration.

II. Theory and Background

One of the most overlooked parts to air vehicle design, especially in academic studies, concerns the effects of installation limits and losses on propulsion system performance. The actual installed performance of an aircraft's engines comprises more than its thermodynamic efficiency; the aerodynamics of propulsion cannot be neglected.

A potentially large portion of gross thrust provided by the cycle can be lost through ram drag and total-pressure-recovery effects. If poorly designed, or poorly matched to an engine, these inlet aerodynamic effects could result in a substantial reduction in net thrust. An engine cycle that produces positive "gross thrust" could easily produce negative installed, "net thrust." An illustration of the control volume for the overall installed engine that highlights the effect of ram drag is shown below in Figure 1.

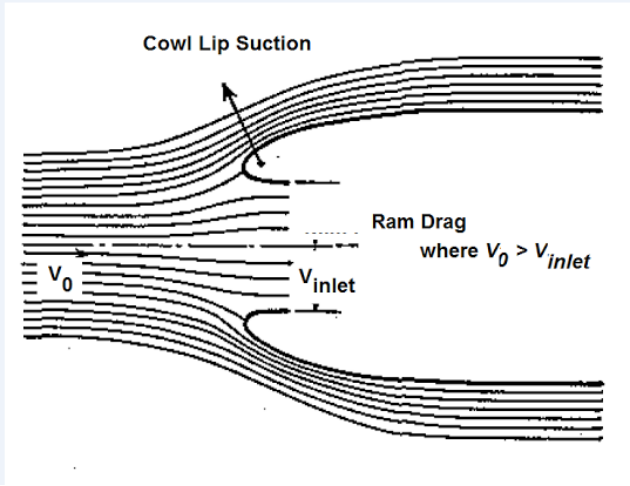

Figure 1 – Illustration Showing the Effect of Ram Drag

In addition, a physical inlet will impose strict limits as to the quality and quanitiy of airflow. These parameters are functions of flight speed, flight altitude, and engine air mass flow demand. If an engine attempts to demand more mass flow than the inlet can provide, the inlet will effectively throttle the engine. Under some circumstances, this effect will manifest itself as a loss of pressure recovery; in other circumstances, the inlet flow will become so uneven to the point that the engine can no longer operate (this is known as the "distortion limit" of an inlet). [13] At other times, if the inlet naturally flows more air than the engine demands, the reduced flow rate will cause free stream air that would otherwise want to enter the inlet to flow around the inlet. This effect creates "spillage drag;" if the flow rates are low enough, the air that actually enters the inlet may become so unsteady as to destabilize engine operation (this is known as the "buzz limit" of an inlet).[13] Thus, the design and size of the inlet may well render unreliable engine operation at many points in the flight envelope. Unreliable engine operation is far worse than inefficient engine operation, as it can lead to engine flame-outs or mechanical failure and a crash.

We will discuss these problems in greater detail, below.

A. The Need for Inlet Diffusion (External Compression)

An additional hardship to the integration of an turbofran engine onto a supersonic airframe is the need to slow the air down to subsonic levels before it hits the compressor. This is due to the fact current technology limits the flow speed a compressor operates under; compressor blades are designed to work on subsonic flows. While a supersonic compressor could theoretically provide very high mass flow rate and pressure ratio per stage, the shockwaves that would form on the blades would result in high losses and making the compressor extremely inefficient.[13] Therefore, in order to have an engine operate at supersonic flight external compression inlets were formalized to ensure that the engine fan face experiences subsonic flow at all flight conditions (subsonic and supersonic).

This paper's main focus is to examine the effect of common external compression inlets have on aircraft performance. The main three topologies are: 1) normal shock inlets, 2) fixed ramp external compression inlets, and 3) variable ramp geometry external compression inlets. See Figure 2 for a sketch of the different geometries.

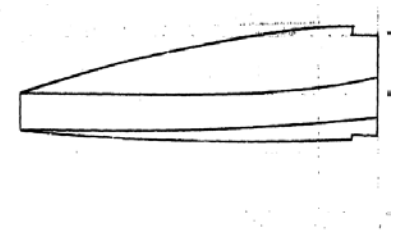

Figure 14. Supersonic Normal Shock Inlet (Second Version)

a

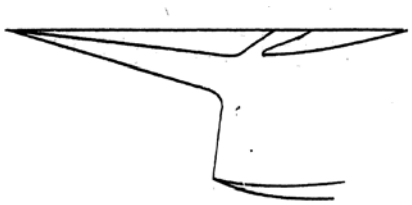

Figure 16. Fixed-Geometry Two-Shock Inlet Design for Mach 1.60

b

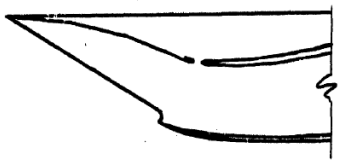

Figure 18. Mach 2.0 Four-Shock Variable-Geometry Inlet

c

Figure 2 – Sketch of Inlet Topologies. a) Fixed Geometry Normal Shock, b) Fixed Ramp External Compression, c) Variable Ramp geometry External Compression (after *PIPSI*[1,2,3,4])

A normal shock inlet is the simplest; see Figure 2a. At subsonic speeds, flow simply enters the inlet. At supersonic speeds, it decelerates flow from subsonic speeds through a single, strong detached "normal shock wave." The drawback to this approach is that there is a stronger overall pressure loss across a normal shock than across a series of oblique shocks.[14] This reduces both the mass flow through the inlet (and hence engine) and also reduces the overall compression ratio (and hence efficiency) of the turbomachinery.

The fixed ramp external compression inlet configuration tries to rectify this pressure loss by understanding that the only isentropic way to go from supersonic flow speeds to subsonic speeds with compression is through an infinite series of oblique shockwaves; see Figure 2b. Similar to its normal shock inlet counterpart, at subsonic speeds, flow simply enters the inlet. The shock waves only form as the vehicle exceeds the speed of sound. However, because the shock formation angle is a function of Mach number, a fixed geometry external compression inlet typically triggers an ill focused collection of crossing shock waves. The pattern of interacting shocks changes with flight speed.

The variable ramp angle external compression inlet configuration tries to improve upon fixed geometry design by including a series of movable ramps. The angles are matched to the flight speed to better coalesce the shock waves across a wide range of supersonic speeds; see Figure 2c. As subsonic speeds, flow simply enters the inlet. Oblique shock waves only form as the vehicle exceeds the speed of sound.

Although ideal, geometry that forms an infinite series of oblique shockwaves (the ideal "isentropic ramp") under all circumstnaces is impossible to design in practice. It can be approximated by a geometry that triggers formation of a finite number of oblique shocks. In comparison to the normal shock inlet, it is possible to greatly reduce the total pressure loss the flow experiences before reaching the compressor of the engine. The weakness of these designs stems from the fact that the delicate structure of oblique shocks can also be disturbed by imperfect flow (such as that associated with a boundary layer). Shock structure is especially disturbed under circumstnaces where the engine does not accept all of the flow supplied by the inlet. Thus, these inlets attempt to better match supply to demand airflow through the inclusion of bypass doors. If the engine does not need all of the air supplied by the inlet, the

excess air is "dumped overboard." These inlets perform poorly, and the shock pattern becomes highly disrupted (or even sucked into the inlet) under circumstances where the engine attempts to demand more airflow than supplied by the inlet.

The drawback to these more complex designs is that they can offset their theoretical effectiveness through the weight, bulk and drag losses associated with moveable ramp, bleed air and bypass doors systems.

The installed, net thrust, $T_{installed}$, is the uninstalled thrust of the engine cycle, less the drag contributions of the aerodynamic losses of installation, *CD*, multiplied by the dynamic pressure, *q*, and normalized by the reference capture area *Ac* of the inlet:

$$T_{installed} = T_{uninstalled} - C_D \cdot q \cdot A_c \tag{1}$$

The external aerodynamic losses applied to gross thrust include the spill effect, bypass and bleed drag:

$$C_D = C_{D_{Spill}} + C_{D_{Bypass}} + C_{D_{Bleed}} \tag{2}$$

B. The Mass Flow Ratio and Distortion and Buzz Limits

The supersonic inlet design problem is dominated heavily by the mass flow ratio the engine experiences. The goal of the design is to have the flow ratio (A_∞/A_c) to be as close to one as possible at the cruise Mach number. This will allow for the propulsion system to perform with the least amount of additional drag possible. For example, if it is performing away from this critical flow ratio, depending on the exact conditions, an inlet will cause the flow of the air to spill around it which will only add to the drag forces the propulsion system produces. Depending on the mass flow ratio, which is shown in Eq. 3, the inlet can operate either critically (where mass flow supply equals the mass flow demanded by the engine), subcritically, or supercritically.

$$MFR = \frac{\dot{W}_{eng}}{\dot{W}_{ideal}} = \frac{A_\infty}{A_c} \tag{3}$$

The ideal conditions, as previously stated, is when the inlet is operating at the critical point, where *MFR=1*. The problems with additional "thrust loss" of the installed engine occur when the inlet is operating subcritically and/or supercritically.

The inlet will be running subcritically when the inlet is supplying more air than the engine actually requires. This is not a crucial problem for inlets with subsonic entry flow or for the supersonic normal shock inlet; mass continuity in the inlet forces the inlet to "spill" excess flow that would under ideal circumstnaces enter the inlet to flow around the whole propulsion system. This drastic change to the flow causes it to change direction sharply in the region of the inlet cowl; it can lead to flow separation outside and inside the inlet. In some cases it could also cause shockwaves to form along the outside of the inlet which would result in even more losses. The distortion of the flow field, and the resulting airframe drag caused by such operation is known as "spill drag," CD_{spill}. Convention has this drag bookkept with propulsive thrust.[15]

For oblique shock external compression inlets (either fixed or variable ramp), the shock structure tends to be delicate. Boundary layer flows forming over inlet ramps will will distort the shock flow field in such a manner that can cause propulsion system instability. In order to provide smoother shock structures, designers build the ramps out of perforated plate (see Figure 3). Because it has experienced isentropic losses as the result of passing through shock waves and the narrow perforated holes, the resulting losses of this airflow are characterized as "bleed drag," CD_{bleed}. Convention has this drag book kept with propulsive thrust.[15]

Figure 3 – perforated plate – inlet bleed on external compression ramp of a McDonnell F-4 Phantom

For oblique shock external compression inlets (either fixed or variable ramp), spillage will distort the shock flow field in such a manner to cause propulsion system instability. Thus, oblique shock inlets cannot reliably function at supersonic speeds when $MFR << 1$; to compensate the inlet system must keep MFR in a narrow range around $MFR \sim 1.0$. To do this, the inlet control system must open up bypass doors to release the air captured by the inlet that cannot be ingested by the engine. While negligible "spill drag" forms under these operating conditions, the air flow "dumped" overboard can distort the flow on the aircraft fuselage. Because it has experienced isentropic losses as the result of passing through shock waves and bypass doors and ducts, the resulting losses are known as "bypass drag," CD_{bypass}. Convention has this drag bookkept against propulsive thrust. [15]

Supercritical operations of the inlet occurs when the the inlet is not supplying the engine the required amount of air it needs. In order to try and correct this deficiency, inlets may feature "suck in doors" that can open for the engine to get a sufficient amount of air. Once again, this mixing of flows causes multiple irregularities leading to additional bypass drag. Suck in doors only function at subsonic speeds. At supersonic speeds, supercritical operation will lead to an unsteady shock wave forming within the inlet.

Another very important effect that needs to be considered is inlet "buzz." This phenonmenon occurs for a large number of supersonic inlets during subcritical operation. An example of this effect is shown in Figure 4 where a shockwave moves from inside the inlet to the tip and then gets sucked back inside.[16] This process is then repeated, creating an osscilation, which causes massive flow disturbances inside the inlet, thus severly damaging engine performance. In some cases this effect can be delayed with the help of boundary layer bleed, although this bleed effect will only increase the overall drag the inlet produces on the engine.[13]

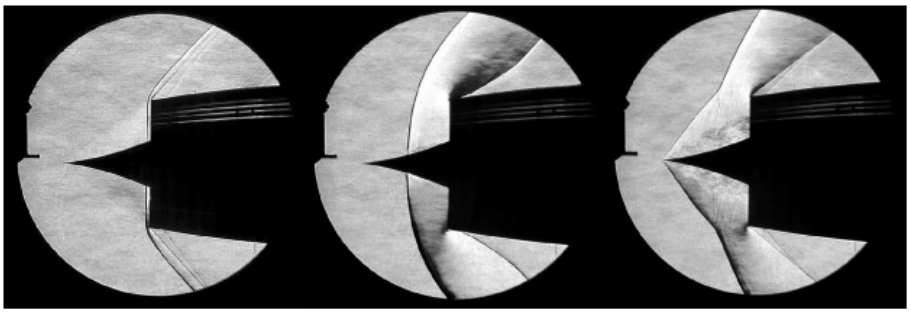

Figure 4 – Schileren Imaging of an Inlet Experiencing Buzz. (see Ref 16)

It is important to nix data points in the event that the inlet is supplying too much or too little air to the engine. The buzz limit is when the engine is operating subcritically; it can cause serious structural damage on top of not allowing the engine to breathe. The distortion limit occurs during supercritical operations; it creates unsteady shockwave inside the inlet. This shockwave can cause serious damage to the flow to the point that it will stop the engine from operating. This occurrence is well known because of the SR-71 Blackbird which inlets were known for their "unstart" problems.[7] Both of these limitations require careful observance in the design of supersonic inlets. Otherwise there will be large gaps in the aircrafts overall flight envelope which could lead to an unflyable aircraft.

III. Analysis Codes and Methods

In order to complete this project, we integrated a variety of engineering codes to simulate the entire aerodynamic and propulsive chain to compute aircraft performance. They ranged from engine simulation to inlet installation as well as aircraft performance calculators. The first tool used in the process was the *Numerical Propulsion System Simulation* (*NPSS*) which is a simulation environment primarily used for engine performance models in aircraft propulsion.[6] The data produced by this tool was then fed into the inlet matching tool designed for this project and based off of the *Performance of Installed Propulsion Systems Interactive* (*PIPSI*) program.[1,2,3,4] Finally, using an energy-manuerverability point-performance designed by the authors the new propusion data was analyzed by being installed in models of a generic F-16 –like combat aircraft.

A. Numerical Propulsion System Simulation (*NPSS*)

NPSS was originally designed by NASA in cooperation with other government agencies to "integrate propulsion technologies with high performance computing and communication technologies into a complete system for performing detailed full-engine simulations."[6] It can run simulations ranging from different propulsion systems to several types of thermal power systems. This program is maintained by a group at the Southwest Research Institute located out of San Antonio, Texas.This group, known as the *NPSS* core project, is focused on updating and fixing any problems with the *NPSS* environment.[17]

In respect to this project, we used *NPSS* along with its built in compressor maps to develop an engine model. The base model was a two-spool subsonic turbofan model as introduced in Gedeon & Takahashi[9,10,11] and expanded later in Dickman & Takahashi[12]. The *NPSS* scripts used in this this study derive from the model used by Dickman & Takahashi.[12] It allows for a parametric variation of four different input variables which include: *BPR, OPR, TIT, FPR*. It incorporates convergence acceleration methods developed by Gedeon[9,10,11] by including an "Up Down Up" scanning procedure. This method varied speed, altitude, and power setting and showed significant improvement over the traditional "up up" nested for-loop structure.

We developed customized models for a variety of different low-bypass ratio turbofan engines (*BPR* =0.5, 1.0 and 1.5) by incorporated inlet topology specific pressure recovery tables. Following *PIPSI*,[1,2,3,4] the pressure recovery at the inlet fan face was implemented as an approximate analytical function of Mach number. Distinct equations were developed to represent the simple normal shock, fixed ramp external compression, and variable ramp external compression inlet configurations. For both the fixed and variable geometry external compression inlets we set the reference mass flow ratio, *MFR* to ~0.8. Meanwhile, for normal shock inlets, we set the reference *MFR* to ~0.9. The resulting curve fits are found in Figures 5a-c.

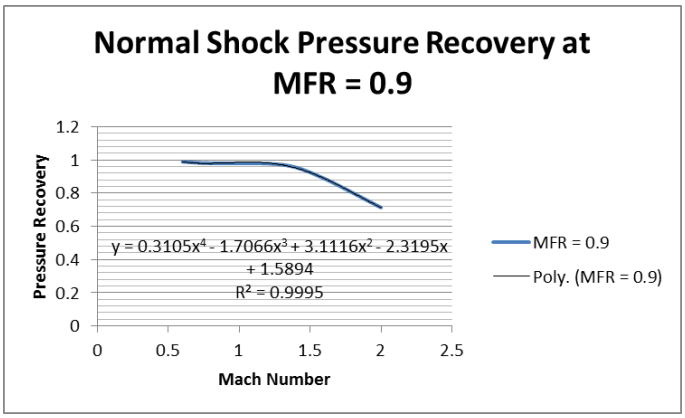

a

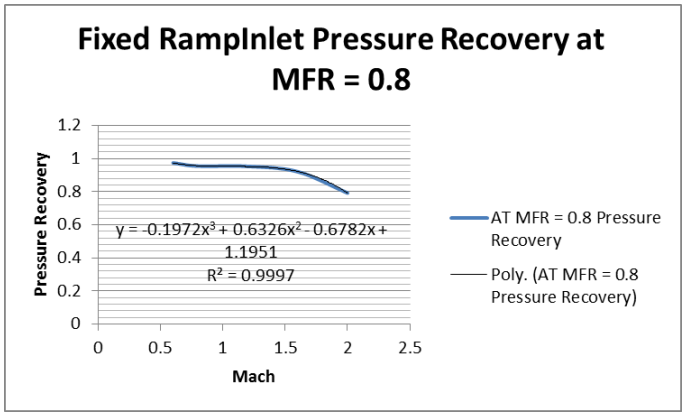

b

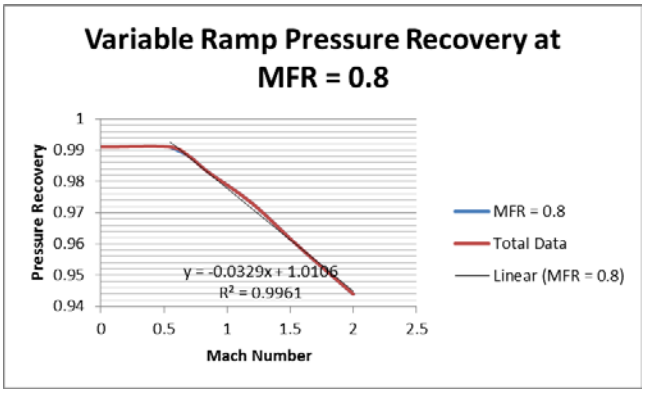

c

Figure 5 – Pressure Recovery models; a) normal shock b) fixed ramp external compression, c) variable ramp geometry external compression

In order to get a good idea of how the various engine parameters (*BPR , OPR, FPR, TIT*) impact the performance of the aircraft, we ran *NPSS* at the following parameters (see Table 1).

Table 1. Engine Parameter Matrix

Parameters	Baseline	Higher *BPR*	Even Higher *BPR*	Lower FPR	Higher FPR	Lower TIT	Lower OPR
BPR	0.5	1.0	1.5	0.5	0.5	0.5	0.5
FPR	1.8	1.8	1.8	1.7	1.9	1.8	1.8
TIT, °R	2700	2700	2700	2700	2700	2300	2700
OPR	35	35	35	35	35	35	30

To have a realistic range of engine data, the *NPSS* two-spool turbofan model simulated: 1) the basic engine without afterburner (dry), 2), the basic engine with afterburner applied to both core and bypass flow. For both dry and reheat operation, we varied core fuel flow from *PLA=-20* (idle) to *PLA=50* (which corresponds to either a maximum *T4* or stoichiometric limit depending upon flight Mach and altitude). We modelled several levels of afterburner fuel flow, from a nominal, minimum fuel flow case through stoichiometry. Both the throat and the nozzle exit area were varied at the off-design points depending on the four engine parameters. This variation kept the engine properly back pressured. This range of engine power levels coupled with a range of Mach numbers from 0 to 2.0 and altitutde from 0 to 60,000 feet gave enough data to produce a wide range of realistic results. We later sort and filter these results to produce a single "power hook" from idle to maximum afterburner.

B. Inlet Matching Using Performance of Installed Propuslion Systems Interactive (*PIPSI*)

This custom tool was critical to understanding the effect installed propulsion has to aircraft performance. It was originally designed by Dickman & Takahashi[12], but was futher improved upon by the Palma to include matching for normal shock inlets, fixed ramp external compression inlets, and variable ramp geometry external compression inlets. The data for each inlet was acquired from *PIPSI*.[1,2,3,4]

PIPSI is a compendium of generic inlet test performance data prepared by Boeing for the USAF. Its purpose was to provide representative data to support trades exactly like this one. *PIPSI* contains sufficient data to correct uninstalled propulsion performance data to account for a wide variety of inlet and nozzle/aftbody installation effects associated with supersonic inlet design[1] Inlet performance losses accounted for by *PIPSI* include spill drag, bleed drag, and bypass drag. *PIPSI* also provides a detailed account of the pressure recovery at various Mach numbers and *MFR.* As previously stated, we utilized these pressure recovery plots in our *NPSS* model.

Our customized tool integrates the tabular data provided in *PIPSI* to establish bypass, bleed and spillage drag corrections as well as determine the buzz and distortion limits which preclude continuous engine operation. We can therefore perform trades whereby any given engine can be fitted with various inlet sizes in order to determine the optimium inlet size and topology for aircraft performance.

We selected three different inlet maps from PIPSI Volume 4 to study the effect of propulsion installation on both military and commericial supersonic aircraft.[4]

The first configuration was "Inlet Configuration #6 – Supersonic, Normal Shock Inlet." According to *PIPSI*, this inlet has no boundary layer bleed or bypass system; the cowl lips are sharp, for reduced drag at higher supersonic Mach numbers. The actual inlet maps are shown below in figures 6a, 7a, 8a. The digitized version of these plots as well as the geometry for this inlet as well as the others can be found in Appendix A.

The next inlet that was analyzed was "Inlet Configuration # 7 – Fixed Geometry, Two-Shock Inlet." a fixed geometry two-shock inlet. It has a seven degree external ramp compression and is equipped with a throat slot for boundary layer bleed. Other noticeable characteristics of this inlet are its sideplates are cutback 75% and has a bleed air dump in its convergent nozzle. The actual inlet maps are shown below in Figures 6b, 7b, 8b

The final inlet strucutre that we anaylyzed is "Inlet configuration #8 – Variable Ramp Geometry, Four-Shock, Two-Dimensional, External Compression Inlet." This is a four-shock, two dimensional, external compression inlet. It has

both a bypass system and a bleed air system which is located aft of the shock. The actual inlet maps are shown below in figures 6c, 7c, 8c.

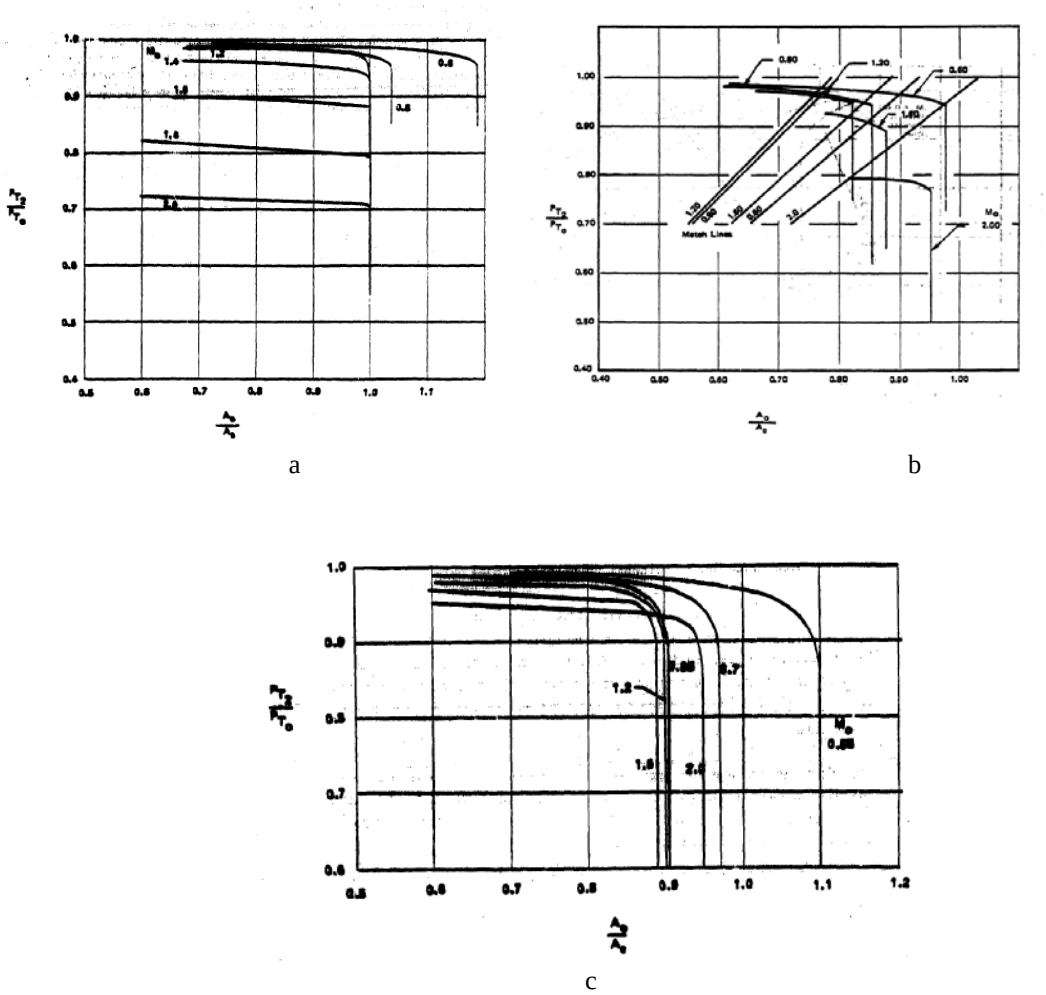

a b

c

Figure 6 – *PIPSI* Performance Characteristics: Pressure Recovery as a function of Mach and Mass Flow Ratio. a) Normal Shock, b) Fixed Ramp Geometry External Compression Inlet c) Variable Ramp Geometry External Compression Inlet (after PIPSI[1,2,3,4])

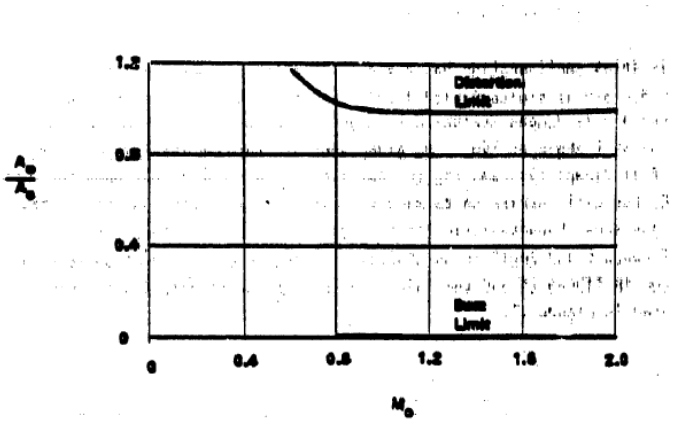

a

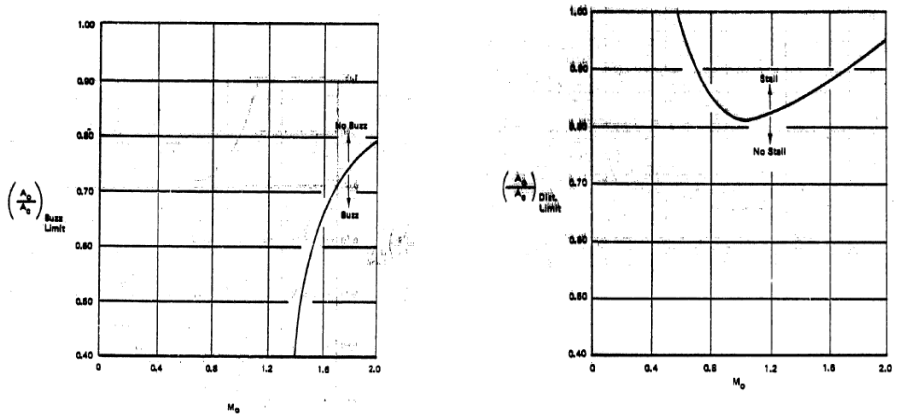

b

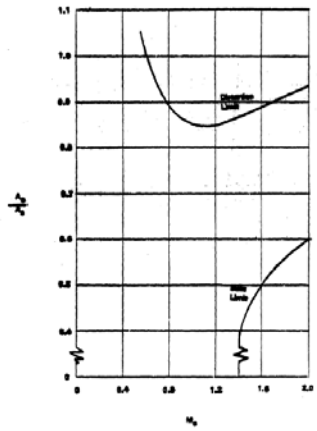

c

Figure 7 – *PIPSI* Performance Characteristics: Buzz and Distortion Limits as a function of Mach and Mass Flow Ratio. a) Normal Shock, b) Fixed Ramp Geometry External Compression Inlet, c) Variable Ramp Geometry External Compression Inlet (after PIPSI[1,2,3,4])

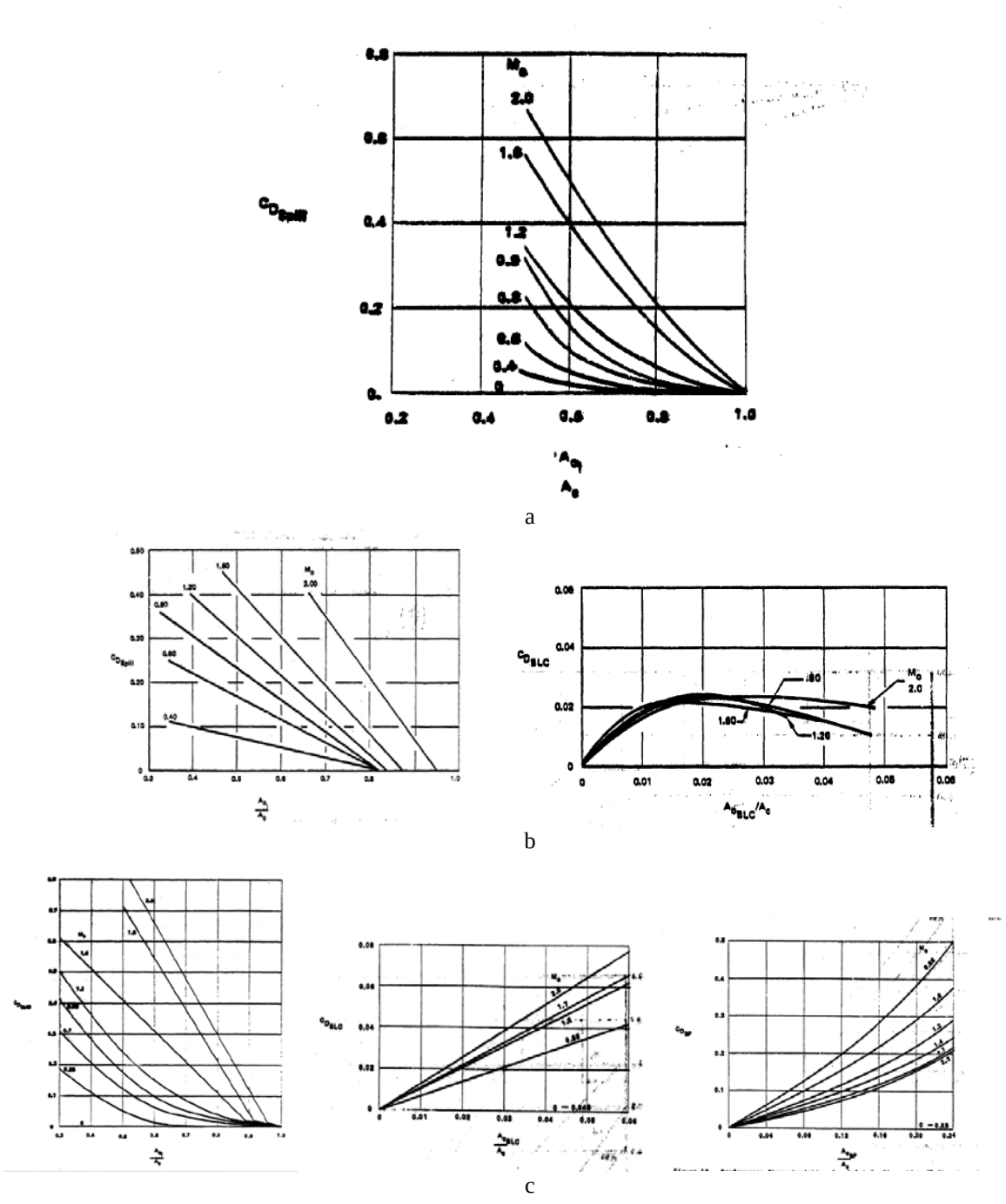

Figure 8 – *PIPSI* Performance Characteristics: Drag Characteristics as a function of Mach and Mass Flow Ratio. a) Normal Shock (Spill), b) Fixed Ramp Geometry (Spill and Bleed) c) Variable Ramp Inlet Geometry (Spill, Bleed, and Bypass) (after PIPSI[1,2,3,4])

After the engine *NPSS* data was corrected using the inlet matching tool, we sorted it into a set of five column data. The first step in doing this was to stitch together the three different *NPSS* models (dry engine, low afterburner, and high afterburner) into one complete engine file. To do this, the tool normalized the *PLA* from 0.01 to 2, where a *PLA*=1 occurs at the maximum thrust dry engine setting. For afterburner settings, we begin with a part-power core setting with minimum afterburner fuel that just exceeds maximum dry thrust. We progress through to *PLA*=2, where the core is running at full power and the afterburner set to maximum (near stoichiometry). This new set of *PLA* was one column in the new data set. The other four columns of data were Mach number, altitude, thrust, and *tsfc*. Together, with the help of interpolation, these five columns allowed for a complete understanding of how the engine operates over the entire flight envelope of an aircraft.

C. Emprical Drag Estimation Technique (*EDET*)

EDET was originally designed for NASA by Feagin & Morrison at Lockheed-California.[18] This old FORTRAN code has been modified to run on a modern PC. It is used to predict reasonable drag values for aircraft based upon basic geometric specifications. From simple top-level geometry, *EDET* develops tables of lift coefficient and drag coefficient as a function of Mach number and angle-of-attack over a wide variety of Mach numbers. It also predicts the Reynolds Number dependent lapse of skin friction associated with flight above or below a specificed reference altitude. *EDET* derives its transonic drag rise from a variety of semi-empirical tables; these are Mach and angle-of-attack dependent functions of wing thickness, sweep and aspect ratio. It also includes a Mach number dependent drag rise model based on the fineness ratio, and effective base area of the fuselage.

EDET is widely used in conceptual design trades as it is the default aerodynamics model in NASA's *FLOPS* code.[19] While its drag numbers are generally considered credible, it remains a concept-design-fidelty code that can only produce an approximate estimate of the drag of any specific configuration.

For this study, we utilized *EDET* to predict the aerodynamics of a generic fighter aircraft, reminiscent of an early production F-16, for purposes of providing a basis to understand how different inlets and engines perform in terms of range and rate-of-climb.[20] This aerodynamic model is identical to that used previously in Dickman & Takahashi.[12] We felt that the early F-16 is a reasonable starting model because it represents a successful combat aircraft with reasonable range, excellent climb and manueverbility as well as high top speed. The actual production F-16 uses a normal shock inlet coupled to a low-bypass-ratio turbofan engine. We were curious to see if we could find a performance improvement associated with a change in engine and/or inlet configuration.

Figure 9. F-16 in Flight

D. Skymaps

The final tool used in this study is an Energy-Manuverability Point Performance (Skymaps) tool. This particular version of the algorithm documented by Takahashi[5] was enhanced and extended by Palma; it is capable of estimating various parameters of an aircrafts performance based off of an aircraft's *EDET* output file as well as its propulsion data. In this case the *EDET* Data for the fighter aircraft was processed in conjunction with the "five column propulsion data" created using the custom *PIPSI* inlet matching tool and *NPSS*. While there are multiple parameters this tool can analyze, the two primary concerns of this report are the skymaps of specific range and rate of climb these models create.

In this study we analyze the notional F-16 aerodynamic database at a flight weight W = 25,000-lbm. The thrust is also normalized to T = 16,000 lbf at military power (max core, no afterburner). This will allow for a decent basis to compare each design.

Specific Range is the best measurement to see how fuel efficient the aircraft is because it measures how many nautical miles the aircraft can travel per pound of fuel burned. The equation for *SR* is shown below in Eq. 4.

$$SR = \frac{V_{ktas}(M,Alt)}{D(M,ALT)*TSFC(M,ALT,PLA=cruise)} \tag{4}$$

Note that for cruise conditions thrust is equal to drag which is why drag can be seen in the denominator instead of thrust.

Meanwhile, the unaccelerated Rate of Climb is a great measurement of excess power the engine develops over the airframe drag. One of the reasons, this is such a valuable measurement is that it gives someone a good sense of how capable the aircraft is able to climb; we can also use it to determine the top speed and/or altitude of an aircraft.

$$RoC(M,ALT) = \ 101.3 * \frac{T(M,ALT,PLA=MAX)-D}{W} * V_{ktas} \tag{5}$$

IV. Results

Each engine was run at different areas for each inlet type. The following inlet's radius were used in the experiment: 0.4 ft, 0.6 ft, 0.8 ft, 0.95 ft, and 1.1 ft.

Table 2. Inlet Size Matrix

Bypass Ratio	Nominal NPSS Engine			Normalized Scaled Engine for Performance Analysis	
BPR	S/L Static Thrust (dry)	Inlet Radius (ft)	Inlet Area (in^2)	S/L Static Thrust (dry) (lbf)	Inlet Area (in^2)
0.5	6350	0.4	72	16000	182
0.5	6350	0.6	163	16000	410
0.5	6350	0.8	290	16000	730
0.5	6350	0.95	408	16000	1029
0.5	6350	1.1	547	16000	1379
1.0	5725	0.4	72	16000	202
1.0	5725	0.6	163	16000	455
1.0	5725	0.8	290	16000	809
1.0	5725	0.95	408	16000	1141
1.0	5725	1.1	547	16000	1530
1.5	7050	0.4	72	16000	164
1.5	7050	0.6	163	16000	370
1.5	7050	0.8	290	16000	657
1.5	7050	0.95	408	16000	927
1.5	7050	1.1	547	16000	1242

A. Max Thrust and Power Hook

We begin by presenting "skymap" plots of the usable flight envelope of the notional combat aircraft in terms of contour plots of maximum thrust in afterburner as a function of Mach and Altitude. For flight envelope regions where the engine and inlet prove mutually incompatible, the engine integration code returns a thrust value of zero (represented by the dark blue regions in the chart). It is important to note that because the fixed ramp geometry inlet behaved similarly to the variable ramp geometry inlet that the plots in the case of BPR = 1.0 and BPR = 1.5 were left out of the document in order to have a better focus on the discussion and to not be unnecessarily redundant.

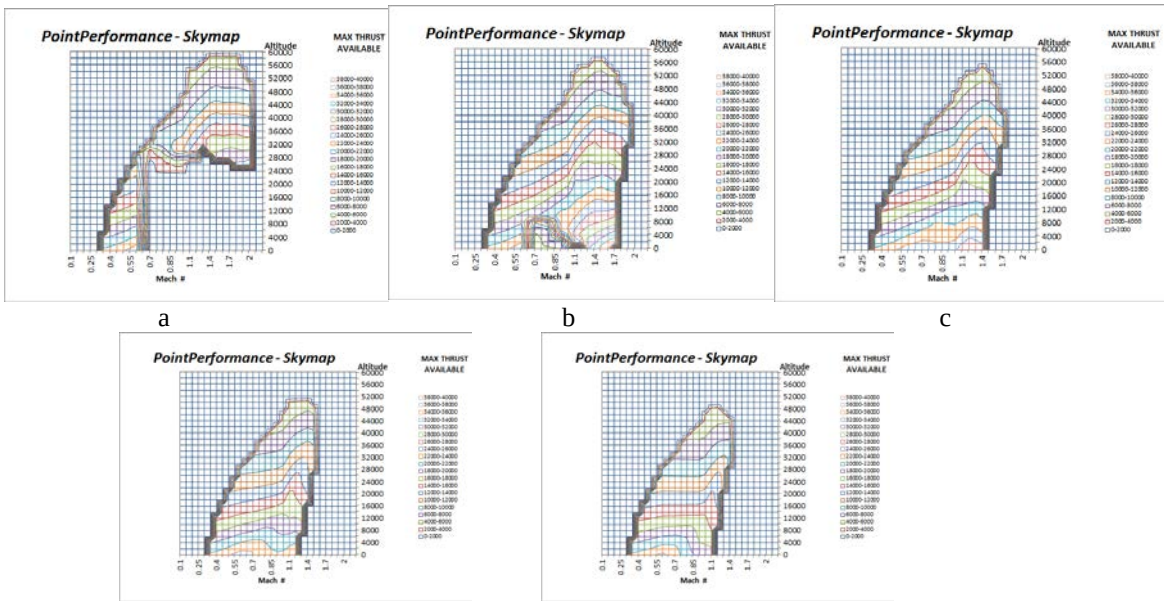

Figure 10 Normal Shock Inlet – Engine Operating Envelope (*BPR* = 0.5): a) R = 0.4 ft; b) R = 0.6 ft, c) R= 0.8 ft d) R = 0.95 e) R = 1.1 ft

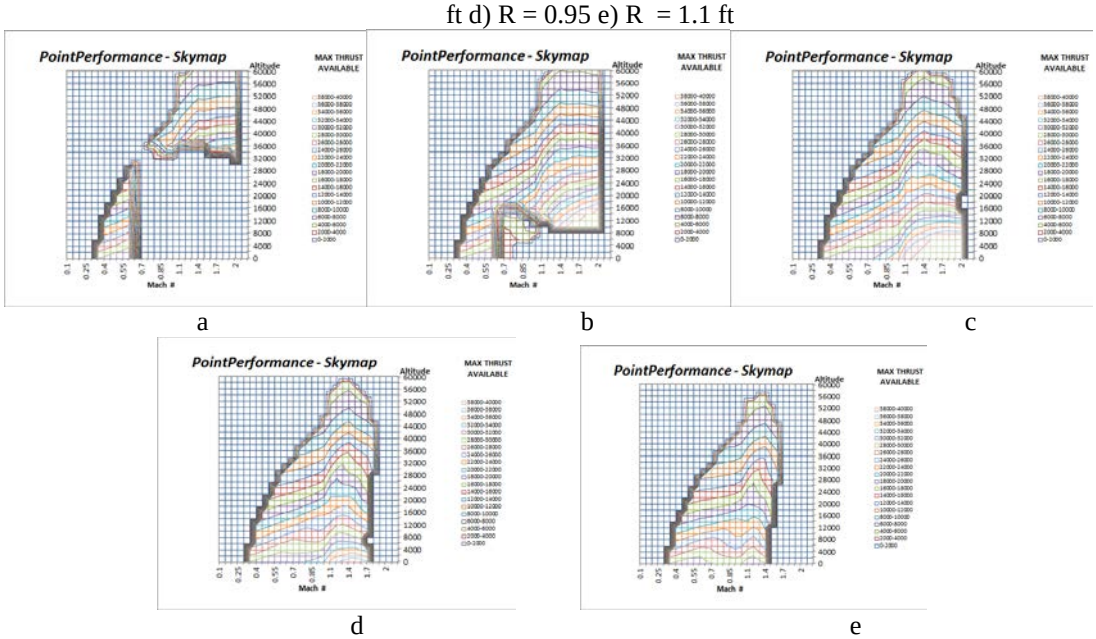

Figure 11 Normal Shock Inlet – Engine Operating Envelope (*BPR* = 1.0): a) R = 0.4 ft; b) R = 0.6 ft, c) R= 0.8 ft d) R = 0.95 e) R = 1.1 ft

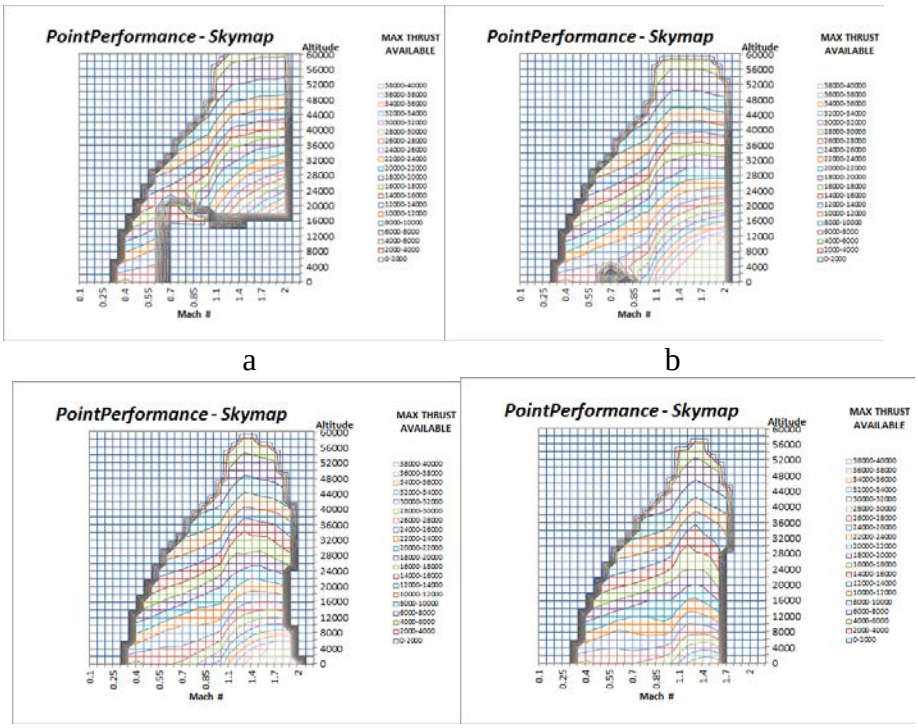

Figure 12 Normal Shock Inlet – Engine Operating Envelope (*BPR* = 1.5): a) R = 0.6 ft b) R = 0.8 ft c) R = 0.95 ft d) R = 1.1 ft

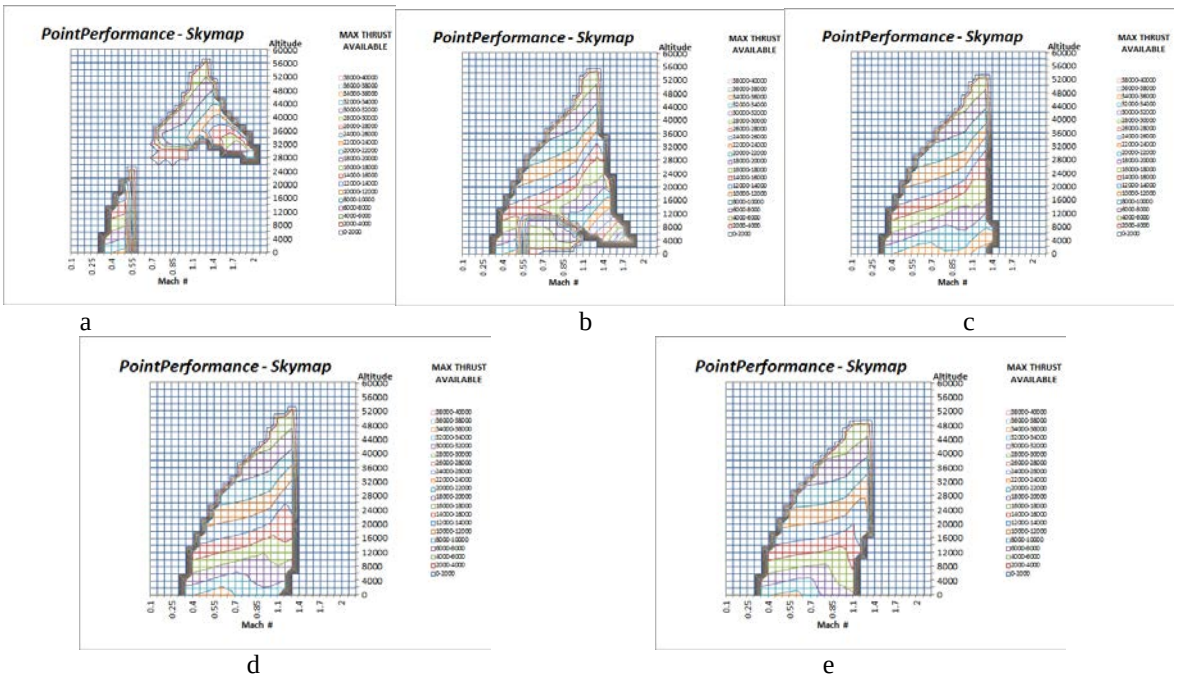

Figure 13 Fixed Ramp Geometry External Compression Inlet – Engine Operating Envelope (*BPR* = 0.5): a) R = 0.4 ft; b) R = 0.6 ft, c) R= 0.8 ft d) R = 0.95 e) R = 1.1 ft

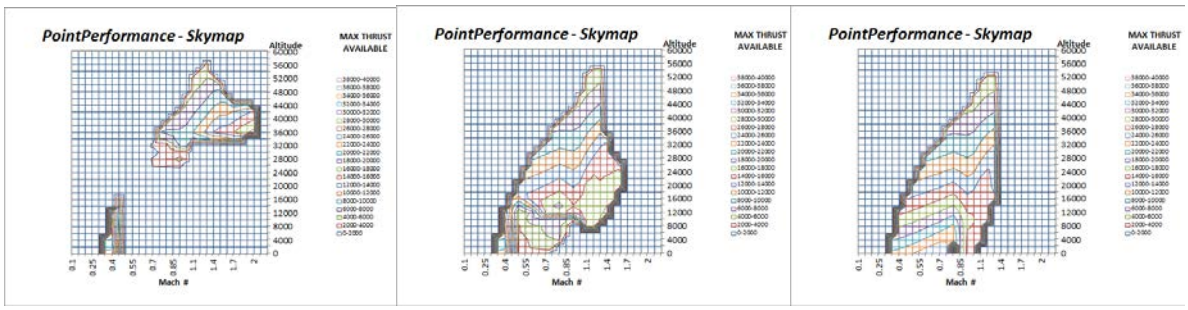

a b c

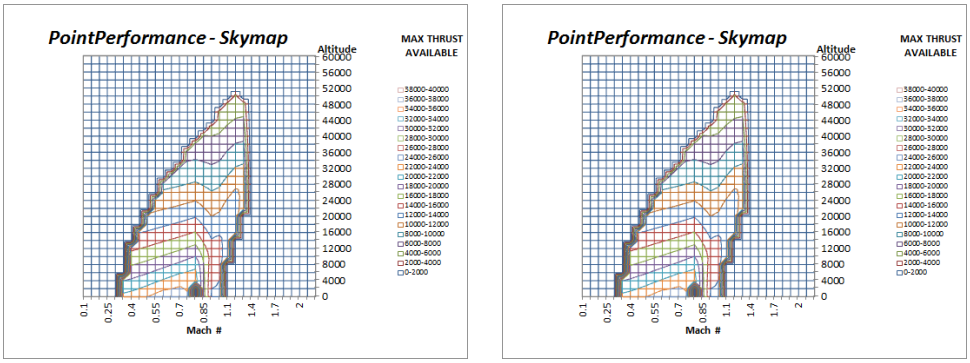

d e

Figure 14 Variable Ramp Geometry External Compression Inlet – Engine Operating Envelope (*BPR* = 0.5): a) R = 0.4 ft; b) R = 0.6 ft, c) R= 0.8 ft d) R = 0.95 e) R = 1.1 ft

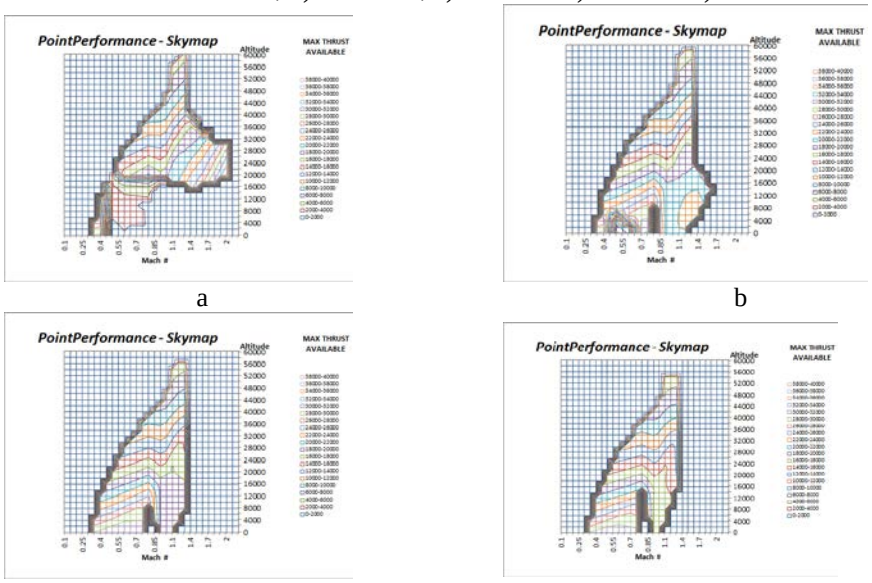

a b

c d

Figure 15 Variable Ramp Geometry External Compression Inlet – Engine Operating Envelope (*BPR* = 1.0): a) R = 0.6 ft; b) R = 0.8 ft, c) R = 0.95 d) R = 1.1 ft

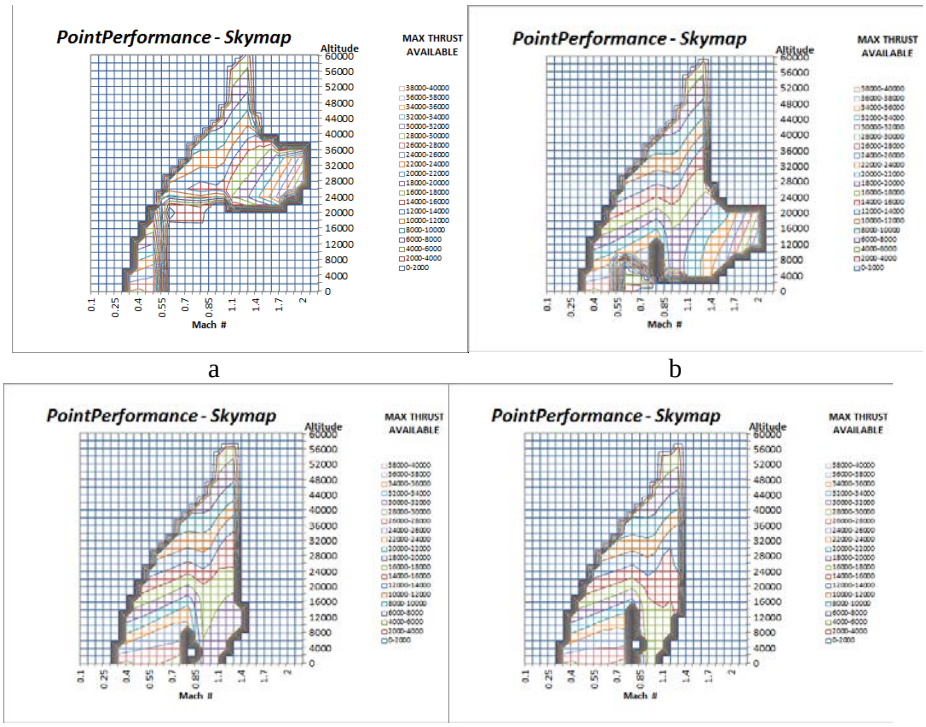

Figure 16 Variable Ramp Geometry External Compression Inlet – Engine Operating Envelope (*BPR* = 1.5): a) R = 0.6 ft; b) R = 0.8 ft, c) R = 0.95 d) R = 1.1 ft

By simply comparing the plots of the same inlet at various *BPR* (Figure 10, 11, 12) we can infer new insight. It is very clear that the range of usable thrust for normal shock inlet makes it extremely versatile. While the engine operating range is severely truncated for the smallest studied inlet (R=0.4-ft), the engine runs well under all larger inlets. Meanwhile, both the fixed and variable ramp geometry inlet appear to have major holes in their flight envelope for a large number of inlet sizes (Figures 13-16). Looking closer at the data, these holes can be explained by both the buzz limit and distortion limit these inlets have which causes the engine to be inoperable at these points. At smaller inlet areas it appears that the supersonic inlet problem is dominated by the distortion limit. However, as the inlet increases the problem shifts from the distortion limit to the buzz limit. This can be observed clearly in Figures 13 and 14 where at the smaller inlet sizes the large chunk of the lower altitudes is largely inoperable. As the inlet increases in size the operating conditions at lower altitudes comes back, but at higher altitudes the performance starts to go away. The buzz limit entirely destroys the flight envelope of the variable ramp inlet past Mach 1.4 once the engine becomes to large. A result of this causes the fixed and variable ramp inlet types to be extremely finicky about their size. The main factor giving the normal shock inlet factor a more diverse operating range is that it has no buzz limit which can be observed in the *PIPSI* charts shown in Figure 7. This allows the normal shock inlet to have a major advantage over its more complex counterpart.

Another phenomenon to notice is that the normal shock inlet actually produces more thrust than its variable ramp counterpart. It is believed that this is caused by two primary sources. The first source is that the buzz limit prevents the variable ramp geometry from actually working past Mach 1.4. This then causes it to not have the added benefit that the normal shockwave inlet experiences at Mach 2 due to pressure differences. The other basis of this difference is that the normal shock inlet does not have any bypass or bleed air drag. Both of these drags account for a majority of the losses of the actual engines thrust.

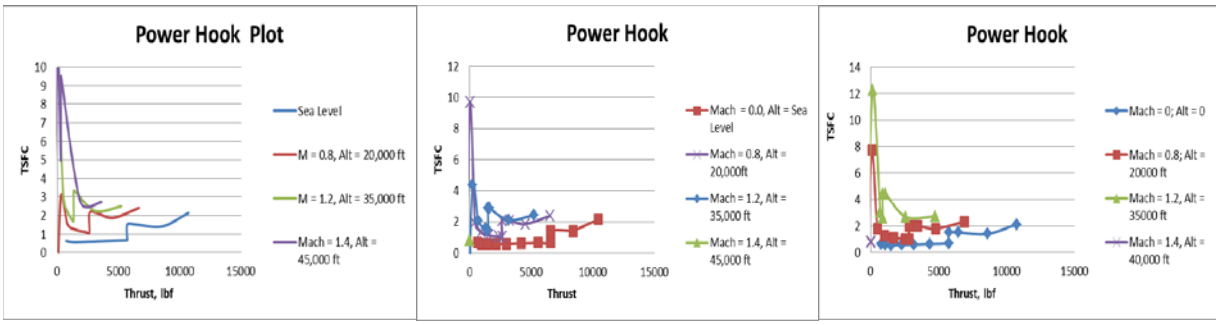

a b c

Figure 17 Power Hook Plots – (*BPR* = 1.0, R = 0.95 ft): a) Normal Shock; b) Fixed Ramp Geometry External Compression Inlet c) Variable Ramp Geometry External Compression

Figure 17 shows the various types of inlets at different mach numbers and altitudes. In these plots the vertical axis is the thrust specific fuel consumption and the horizontal axis is the thrust produced at each *PLA*. The major takeaway from these plots is that it is very evident once again that the normal shock inlet is capable of flying at Mach 1.4 at an altitude of 45,000 feet while both the fixed and variable ramp inlets are not. Also, it would appear that there is almost no difference in the TSFC between the normal shock inlet and its more complex counterparts. This tends to show that the simpler design maybe better even though it does not have as good of a pressure recovery as the the fixed ramp and variable ramp designs.

B. Specific Range Performance

In a continued effort to understand the different benefits each inlet has the skymaps tool was then used to compare the specific range of the generic F-16-like airframe when it is equipped with the different inlets. This comparison allows for a good understanding of how inlet changes impact airplan efficiency. In order to have a good representation of the data only plots that had a good overall flight envelope were kept. This allows for a reasonable assessment of the performance of the two inlets.

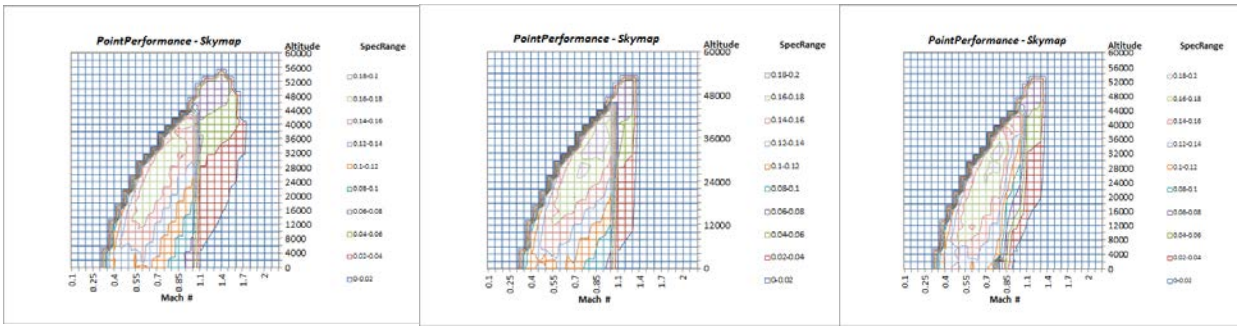

a b c

Figure 18 Specific Range of Various Inlet Designs – (*BPR* = 0.5, R = 0.8 ft): a) Normal Shock; b) Fixed Ramp Geometry External Compression Inlet c) Variable Ramp Geometry External Compression

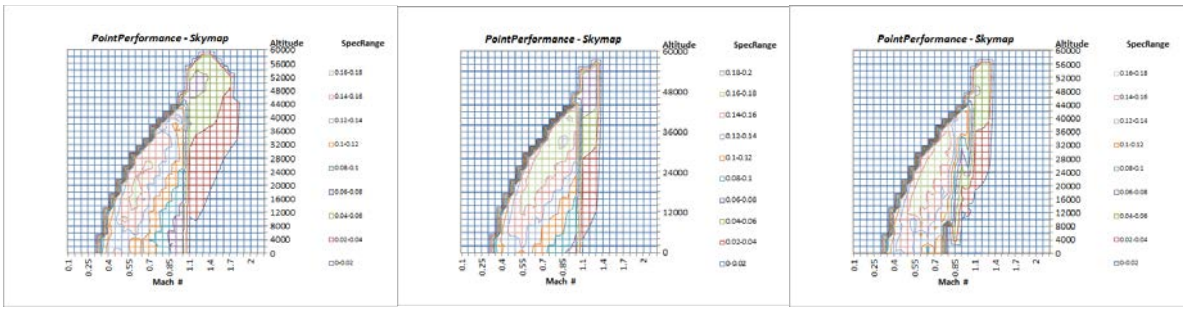

a b c

Figure 19 Specific Range of Various Inlet Designs – (*BPR* = 1.0, R = 0.95 ft): a) Normal Shock; b) Fixed Ramp Geometry External Compression Inlet c) Variable Ramp Geometry External Compression

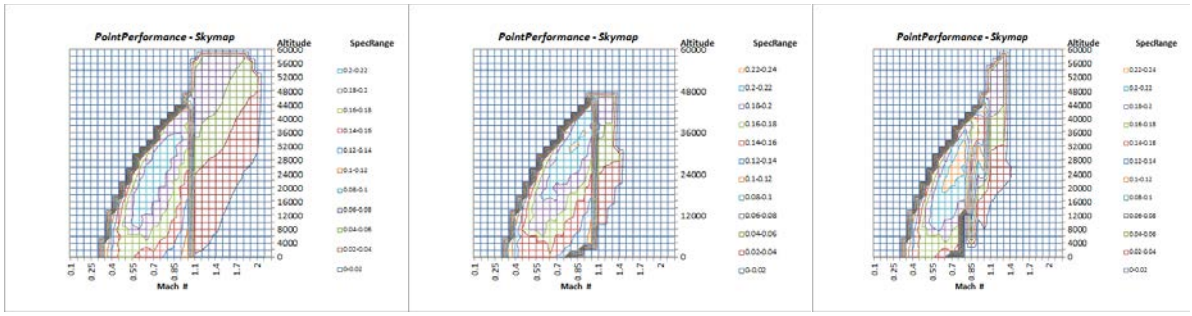

a b c

Figure 20 Specific Range of Various Inlet Designs – (*BPR* = 1.5, R = 0.8 ft):a) Normal Shock; b) Fixed Ramp Geometry External Compression Inlet c) Variable Ramp Geometry External Compression

Before looking at the differences between the three different inlet geometry the authors of the paper made an observation between the correlation of inlet size and specific range. We observed that, regardless of the inlet type, as the size of inlet grew the specific range of the aircraft decreased for a constant *BPR* . This is an important concept to understand when designing an inlet. The inlet needs to be made large enough to account for any distortion limits, but kept small enough so its performance is not greatly reduced even if it still has a large flight envelope at larger sizes.

After studying Figures 18, 19, and 20 it is clear that the more complex fixed and variable geometry inlets do have a better fuel consumption, but at a significant cost. For every fixed and variable ramp inlet size that produced a strong looking flight envelope, the F-16 was incapable of flying past Mach 1.4. For many other possible inlet sizes, the distortion and buzz limits precluded any engine operation over a large range of Mach / Altitude space. While it does clearly have better performance shown strongly in Figure 18, the inablility to fly faster than Mach 1.4 is a major concern. This could add to the reason the F-16 is fitted with a normal shock inlet instead of a theoretically better performance inlet such as the variable ramp inlet. Of course, the variable inlet could be designed so it can perform at desired design conditions, but not without gutting its flight envelope. This is a major problem because the off-design is just as important as the actual design point for airplanes. In the case of military planes they need to be able to maneuver at various altitudes and Mach numbers without fear of any engine buzz or distortion limits. Meanwhile, commercial airplanes have to be strongly tested in the event of any scenario and it would be hard convince a certification authority such as the FAA to approve of such an aircraft when such large “chunks” of the flight envelope are missing due to propulsion deficiencies.

C. Rate of Climb Performance

The final criteria of the airplane performance that is analyzed is its rate of climb performance. This statistic allows for a good insight into how well this airplane is able to accelerate and maneuver in terms of climbing. Similar to the specific range only plots with a reasonable flight envelope were kept. Again this should allow for a good analysis of the data without being mislead by the performance of inferior inlets.

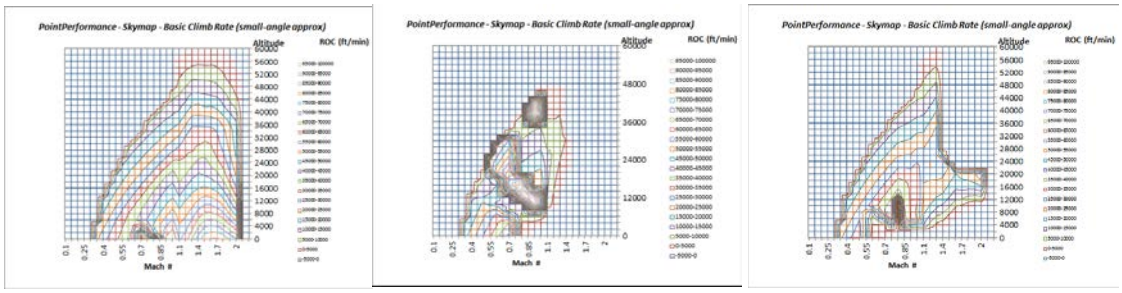

a b c

Figure 21 Rate of Climb with Various Inlet Designs – (*BPR* = 1.5, R = 0.8 ft): a) Normal Shock; b) Fixed Ramp Geometry External Compression Inlet c) Variable Ramp Geometry External Compression

One thing to notice about the plots is that the variable ramp inlet limits the overall performance once again at higher speeds. If designed right it can reach flight speeds close to Mach 2, but at the cost of a large portion of the flight envelope missing. The fixed ramp geometry inlet also shows this problem, but is not nearly as affected as its variable geometry counterpart. Meanwhile, once again the normal shock inlet appears to have no issue as the *BPR* increases. This robust nature of the normal shock inlet leads the authors to believe that it may be a superior choice in th inlet design.

D. TIT, FPR, OPR Trade Studies

For simplicity and in order to have a better understanding of how the other engine parameters FPR, OPR, and TIT affect the performance of an aircraft the trade studies were only done using a normal shock inlet with a radius of 0.8 ft. Refering back to table 1 the trade studies run for this include lowering the *TIT*, both increasing and decreasing the *FPR*, and decreasing the *OPR*. Table 3 below shows the various scaling of each new engine and how scaling to the normalized value of 16,000 lbf has on the size of the engine

Table 3. Inlet Size Matrix for TIT, FPR, OPR Trade Studies

Bypass Ratio	Turbine Inlet Temperature	Fan Pressure Ratio	Overall Pressure Ratio	Nominal NPSS Engine			Normalized Scaled Engine for Performance Analysis	
				S/L Static Thrust (dry)	Inlet Radius (ft)	Inlet Area (in^2)	S/L Static Thrust (dry) (lbf)	Inlet Area (in^2)
BPR	TIT °R	FPR	OPR					
0.5	2700	1.8	35.0	6350	0.8	290	16000	730
0.5	2300	1.8	35.0	6725	0.8	290	16000	689
0.5	2700	1.7	35.0	6325	0.8	290	16000	732
0.5	2700	1.9	35.0	6340	0.8	290	16000	731
0.5	2700	1.8	30.0	6370	0.8	290	16000	727

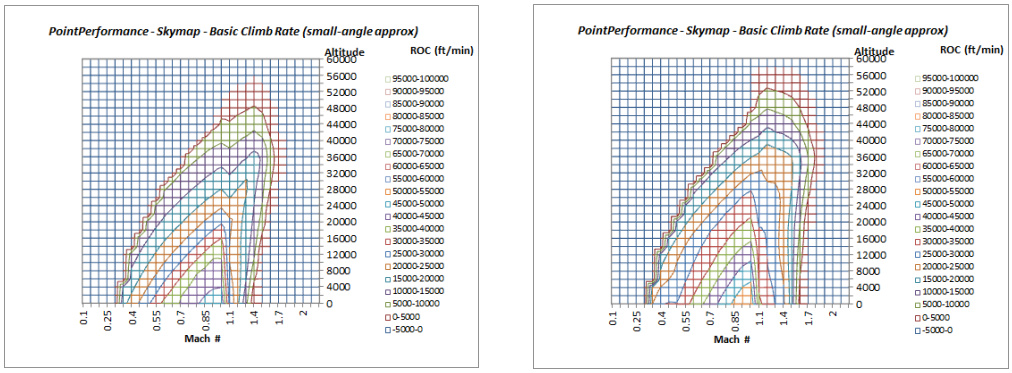

a b

Figure 22 Normal Shock Inlet –Engine Operating Envelope – Rate of Climb R=0.8 ft, OPR = 35, BPR = 0.5, & FPR = 1.8 a) TIT = 2700 °R; b) TIT = 2300 °R

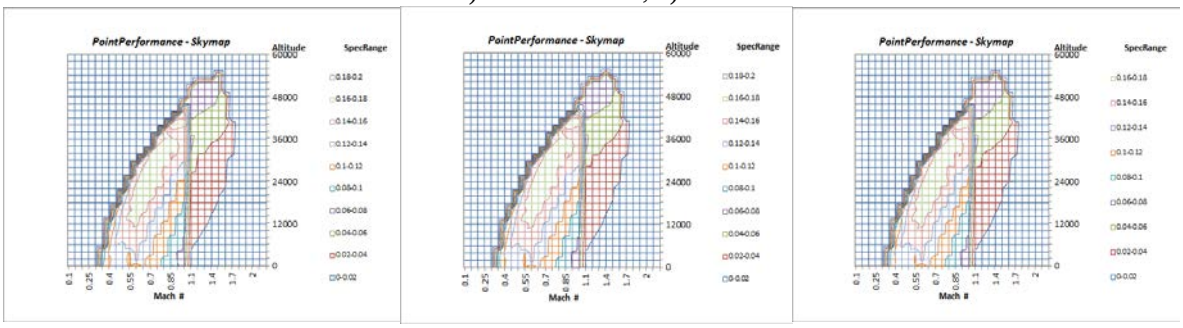

a b c

Figure 23 Normal Shock Inlet – Engine Operating Envelope – Specific Range R=0.8 ft, OPR = 35, BPR = 0.5, TIT= 2700 °R a) FPR = 1.7; b) FPR = 1.8; c) FPR = 1.9

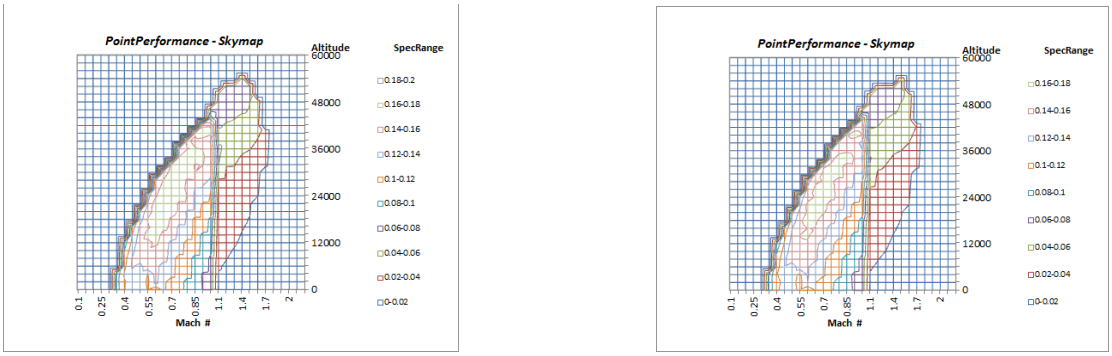

a b

Figure 24 Normal Shock Inlet – Engine Operating Envelope – Specific Range R=0.8 ft, BPR=0.5, TIT=2700 °R a) OPR = 35; b) OPR = 30

By comparing Table 3 with Figures 22 – 24 several interesting conclusions can be made by varying the various engine parameters. To begin with, it is clear that by looking at Table 3, when the TIT is decreased the dry sea level static thrust is actually increased. When computing the fuel flow of the engine in the Skymaps algorithm it is multiplied by the engine scale factor. Therefore, in order for an engine to have a lower fuel flow it would be wise to have the base thrust level be as high as possible. This is especially important for aircraft such as commercial planes to pay attention to an engines TIT to help decrease their fuel flow as much as possible. Another factor to notice in these plots is that the OPR has a pretty large impact on the specific range of the aircraft. Taking a close look at Figure 24 it would appear that as the overall pressure ratio is lowered, the specific range of the aircraft is also decreased. This would mean that a high overall pressure ratio would be favorable for aircraft that rely on burning the least amount of fuel over long range missions. The downside to having the increased *OPR* for an engine is that it

appears that it ever so slightly loses the ability to fly in some of the outer edges of the envelope compared to an engine of a lower *OPR*. This can be seen most prominently by looking at the very outermost right edge of red in the supersonic regime. In Figure 24a it is clear that the plateau of red is much shorter vertically and does not stretch as far as the case in 24b. Finally, analyzing the change in *FPR* also yielded several subtle, but fascinating results. For example, while the overall envelope changes very little it is clear that by increasing the parameters value that it does have a small change on the specific range of the aircraft. As *FPR* increases the specific range decerases yielding a inverse relationship between the two parameters. However, as *FPR* changes it also has a very subtle affect on the actual flight envelope of the aircraft itself. For example, looking near the top of the flight envelope it does change the available areas where the F-16 model is capable of flying. In fact, it would appear that it ever so slightly allows it fly higher as *FPR* increases. This can be seen in Figure 23c with the sharp vertical increase in the flight region of the supersonic area compared to the gradual increase of the flyable area. Therefore, it is important to find a decent inbetween value for the aircraft to have a higher specific range, but also a robust flight envelope.

V. Conclusion

Supersonic inlet design is an interesting topic that requires a lot of attention and finding the perfect inlet size based off of the inlet design desired. There is an especially constant give and take with both the fixed and variable ramp inlet that requires a very nuanced design in order to get a valuable performance out of it. In fact, despite it allowing for a better specific range then the normal shock inlet, it may be the inferior choice of the two. The normal shock inlet, if sized properly, allows an aircraft to fly nearly anywhere at any speed. This is especially useful for fighter planes who require a large window of operation. It also allows airplanes that need to be approved by the FAA to have a stronger basis for their design. If specific range is a key design parameter than the difference between the two inlets could be made up by having a larger *BPR* engine. In fact, despite the increased weight caused by the larger engine size, the normal shock would be vastly more simple to design and maintain through an aircrafts lifespan. This could go a long way in making supersonic travel a viable option for everyone which would be a major improvement for millions of people. If the more complicated variable ramp design is to ever truly be utilized to its maximum potential a deeper analysis of the buzz and distortion limits needs to be made. Hopefully, through more research new inlet designs can be achieved to allow for the more fuel efficient inlets without large losses in the flight envelope to become the dominant choice in aircraft design.

Appendix A – Digitized *PIPSI* Plots for various Inlet topologies

1. *Pressure Recovery*

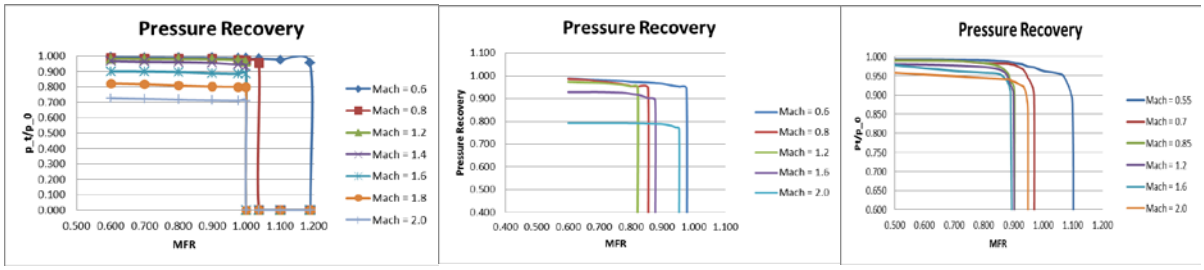

a b c

Figure A-1, Digitized Pressure Recovery of *PIPSI* Charts – a) Normal Shock Inlet b) Fixed Ramp Geometry Inlet
c) Variable Ramp Geomemtry

2. *Buzz and Distortion Limits*

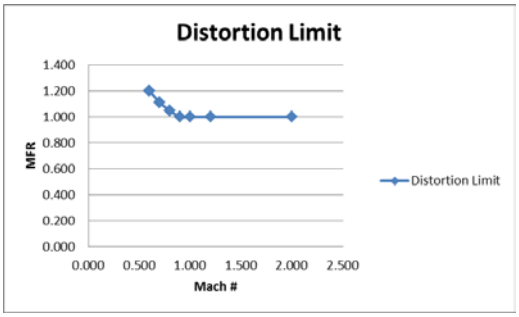

Figure A-2, Digitized Distortion Limit of Normal Shock Inlet *PIPSI* Chart

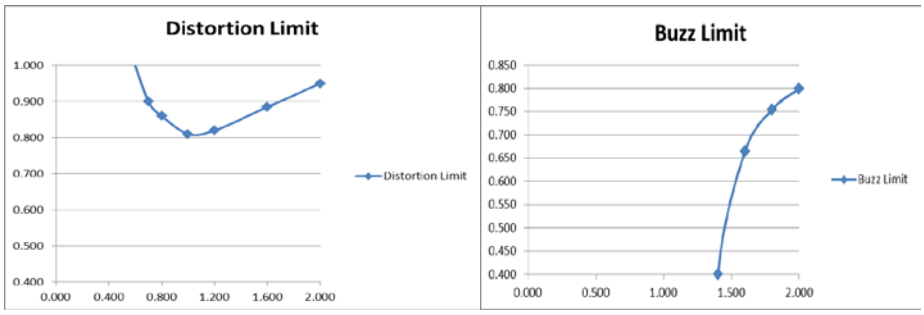

a b

Figure A-3, Digitized Plots of Fixed Ramp Geometry Inlet *PIPSI* Data – a) Distortion Limit b) Buzz Limit

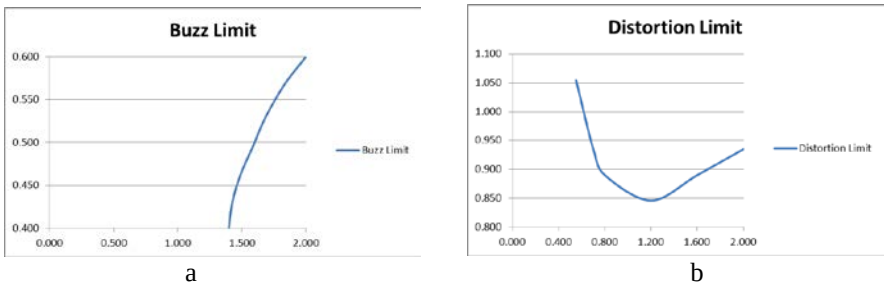

a b

Figure A-4, Digitized Plots of Variable Ramp Geometry Inlet *PIPSI* Data – a) Buzz Limit b) Distortion Limit

3. Drag

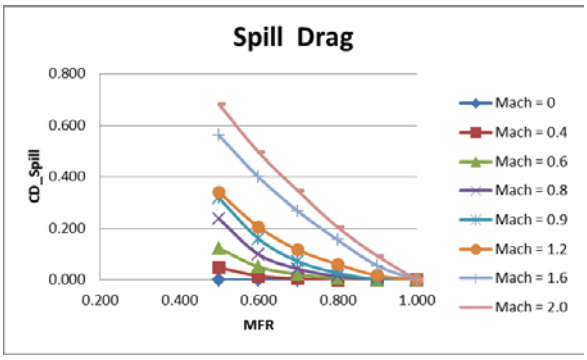

a

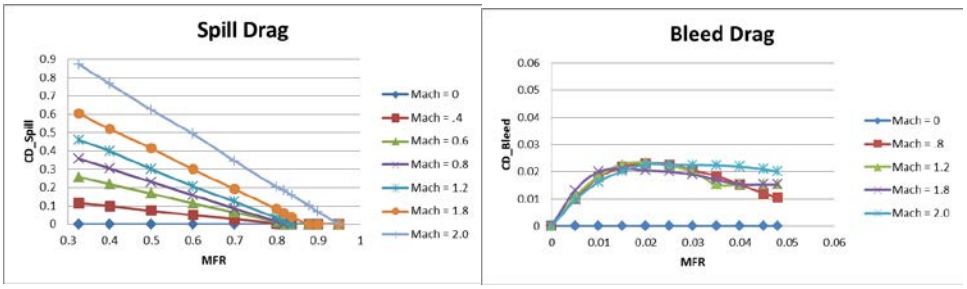

b

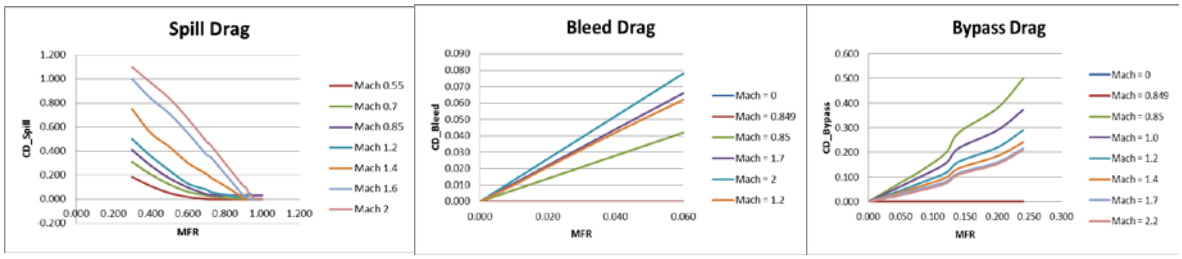

c

Figure A-5, Digitized Plots of Various Inlet *PIPSI* Drag Data – a) Normal b) Fixed c) Variable

Acknowledgments

Mr. Palma developed and extended many tools used to perform this unfunded project in partial fulfillment of the degree requirements for obtaining his M.S. in Aerospace Engineering from Arizona State University. All analysis was completed at Arizona State University with the aforementioned tools: *EDET and NPSS*.

References

[1] Ball, W. H. ; Hickcox, T. E, "Rapid Evaluation of Propulsion System Effects. Volume I," TECHNICAL REPORT AFFDL-TR-78-91, VOLUME I, July 1978.

[2] Ball, W. H. ; Atkins, R.A., Jr., "Rapid Evaluation of Propulsion System Effects. Volume II – *PIPSI* Users Manual," TECHNICAL REPORT AFFDL-TR-78-91, VOLUME II, July 1978.

[3] Hickcox, T. E, R.A. Atkins, Jr. and Ball, W.H., "Rapid Evaluation of Propulsion System Effects. Volume III – Derivative Procedure Users Manual," TECHNICAL REPORT AFFDL-TR-78-91, VOLUME III, July 1978.

[4] Ball, W.H., "Rapid Evaluation of Propulsion System Effects. Volume IV – Library of Configurations and Performance Maps," TECHNICAL REPORT AFFDL-TR-78-91, VOLUME IV, July 1978.

[5] Takahashi, T.T., "Aircraft Concept Design Performance Visualization Using an Energy-Maneuverability Presentation," AIAA 2012-5704, 2012.

[6] NPSS, Numerical Propulsion System Simulation, Software Package, Ver. 2.3.0.1, Ohio Aerospace Institute, Cleveland, OH, 2010

[7] See: *http://www.enginehistory.org/Convention/2005/Presentations/LawPete/SR-71Propulsion1.pdf*

[8] Sóbester, A., "Tradeoffs in Jet Inlet Design: A Historical Perspective," AIAA J. Aircraft Vol 44, No. 3, 2007. pp. 705-717.

[9] Gedeon, C. and Takahashi, T.T., "Multi-Disciplinary Survey of Engine Parameters and the Resulting Impact on Energy Maneuverability," AIAA 2014-2032, 2014.

[10] Gedeon, C. and Takahashi, T.T., "A Multi-Disciplinary Survey of Energy Maneuverability for Subsonic Endurance Based Aircraft," AIAA 2014-3156, 2014.

[11] Takahashi, T.T. and Gedeon, C., "The Effect of Propulsion System Scale and Bypass Ratio Upon Optimum Climb Speed," AIAA 2015-1677, 2015.

[12] Dickman, C. and Takahashi, T.T., "Engine/Inlet Matching for Supersonic Aircraft Design," AIAA SciTech Conference, January 2016

[13] Hill, P.G. and Peterson, C.R., *Mechanics and Thermodynamics of Propulsion*, Addisson-Wesley, 1965.

[14] NACA REPORT 1135, "Equations, Tables and Charts for Compressible Flow"

[15] Numbers, K., "Hypersonic Propulsion System Force Accounting," *AGARD CONFERENCE PROCEEDINGS 31-1*, 1992.

[16] Chima, R.V., "Analysis of Buzz in a Supersonic Inlet," NASA/TM-2012-217612, 2012.

[17] *See:* http://www.swri.org/*NPSS*/

[18] Feagin, R. C., and Morrison, W. D., "Delta Method, An Empirical Drag Buildup Technique," Lockheed-California Co./ Rept. LR-27975-VOL-1, 1978

[19] McCullers, L. A., "FLOPS User's Guide Ver. 5.94," NASA Langley Research Center, Hampton, VA, Jan. 16th, 1998.

[20] See: *http://www.af.mil/AboutUs/FactSheets/Display/tabid/224/Article/104505/f-16-fighting-falcon.aspx*